

Response to Reviewer 1

Many thanks for your insightful comments and careful examination of the manuscript. I have studied your comments carefully and tried our best to revise the manuscript. My responses are given as follows. Attached please find the revised version. Thank you and best regards.

1. [This manuscript describes mathematical research. The application is to a classical hydrological problem but the results are about comparing (theoretical) calculated quantities.]

Response: Many thanks for your insight comments. This manuscript developed a new method to partition the climate and catchment effects on runoff. I think that it is quite reasonable to compare the method with the existing ones.

2. [In more detail, the formulation of the problem addressed in described in detail on pages 2-3 (lines 77-89). The basic idea is that the standard first order expansion for a total differential does not adequately consider the order of the differentiation. A new proposal is made that enables the first order expansion to be used. In short I did not understand the proposed formulation of the problem.]

Response: Yes. Many previous studies have used the first order approximation to evaluate the hydrologic response to climate and catchment conditions, so that they are not mathematically precise. Please see Yang et al (2014) for details.

3. [To my mind this is classical calculus and it may be better to get a professional mathematician to evaluate the work. My own evaluation is that I could not see the underlying point of the formulation. On my understanding (and remembering that I am not a professional mathematician) we use a first order expansion to get the total differential, and each of the individual differentials are considered to be infinitesimal in which it does not matter about the order. If we want more detail then we make a second order expansion, e.g., using the example from the text, i.e., $R=f(x, y)$, we have for the relevant second order term a differential like; $\partial^2 R/(\partial x \partial y)$ to more fully account for the missing part. Such rigour is rarely used in Hydrological (or science) practice since we usually have finite differences (rather than differentials) and the necessary accuracy is usually only 10% or so.]

Response: Yang et al (2014) have shown that the first order expansion has caused an error of the climate impact on runoff ranging from 0 to 20 mm (or -118 to 174%) over China. Although the error is probably trivial sometimes, anyway, a precise method is always desirable.

Reference

Yang, H., D. Yang, and Q. Hu: An error analysis of the Budyko hypothesis for assessing the contribution of climate change to runoff. *Water Resources Research*, 50, 9620–9629, 2014.

Response to Reviewer 2

Many thanks for your insightful comments and careful examination of the manuscript. I have studied your comments carefully and tried our best to revise the manuscript. My responses are given as follows. Attached please find the revised version. Thank you and best regards.

1. [The paper describes a mathematical method to attribute a discrete change in runoff to changes in climate and catchment characteristics. The method is directly applicable to common data and yields quite similar results when compared to existing methods. However, it remains open which of these methods is more accurate because there is no data to verify.]

Response: I admitted that I have not provided data to verify the LI method. However, the method is mathematically precise but the other methods are not, so that it is more accurate than other methods.

2. [Still, there are two interesting and valuable aspects of the manuscript: a) The role of the evolution over time b) Reconciling the existing methods and their assumptions on this evolution]

Response: Many thanks for your appreciation.

3. [To consider the path of changes is an important aspect and, as the author illustrates, may thus alter the resultant sensitivity to a change. This is important, since this may allow to better assess the vulnerability of a given catchment to global change. The problem is, that there is usually not sufficient data to constrain the evolution of disturbances.]

Response: I have added a paragraph to discuss the high data requirement associated with the LI method. See line 316-321 for details.

4. [The author uses subperiods of 7 years, where at least the meteorological data provides some constraints. However, the use of shorter periods comes at the cost of potential changes in the catchment water storage, which can then be misinterpreted as changes in catchment characteristics. Figure 6 shows that the temporal variation of the catchment property sensitivity is largest. This might

actually be caused by water storage changes, rather than actual changes in the catchment properties. This aspect is not sufficiently discussed in the manuscript.]

Response: I have added a paragraph to justify my use of an aggregated time period of 7 years. See Lines 322-338 for details.

5. [Although I like that the existing methods are discussed in detail, I strongly recommend that the author better visualizes these methods. An attempt is done in Figure 1, but this must be extended and linked to the other methods.]

Response: I have revised Figure 1 as you suggested.

6. [Recommendation: Major Revisions. The relevance/significance of the paper must be better highlighted. This requires major changes throughout.]

Response: Thanks for your comments. I highlighted the relevance in lines 39-43, 81-92, 94-98, 313-316, and 339-349.

7. [Further comments: Overall, the notation should be more consistent (for example indices) and streamlined]

Response: I have checked the notation throughout the manuscript.

8. [I think that some parts of the paper can be cut. Figure 2b is trivial and can be removed]

Response: A major conclusion of the manuscript is that the decomposition method is a special case of the LI method. Figure 2b lends direct support to the conclusion so that it is not trivial. I am sorry I do not cut it.

9. [It would be better to describe the decomposition method in a conceptual Figure, similar to Fig.1.]

Response: I have revised Figure 1 as you suggested.

10. [The catchments with the largest changes in n have a reference period of only 3 years. This is quite short for a reference period.]

Response: I am sorry that I directly used the data given in Zhou et al (2016). Many thanks for your careful examination, but the data of the catchment NO.10 remains in the manuscript considering the reasons below: 1) the catchment has a high aridity index of 1.5. In dry areas, the carryover of soil water storage between years is relatively small as much of the annual precipitation is evaporated and thus has little effect in altering water storage. For example, a one-year aggregated time period may be appropriate in the semi-arid Loess Plateau (Ning et al., 2017) ; 2) the carryover of soil water storage would result in an overestimated E , and in turn an overestimated n . The catchment NO.10 had a medium n value (1.7) in the reference period, much smaller than the evaluation period (4.2), so that the largest changes in n cannot be related to the effect of the carryover of soil water storage.

11. [Figure 6: It is unclear what is shown here.]

Response: Figure 6 compares the temporal variability of the sensitivities of water yield to precipitation, potential evapotranspiration, and catchment properties. The boxplot clearly showed that the sensitivities to catchment properties had a much greater temporal variation.

12. [The motivation of the figures 7,8 and 9 is not really clear to me. Please explain or remove]

Response:

Figure 7 shows the correlation of the obtained sensitivities with P , E_0 , n , and aridity index, for purpose to determine the predictors of the sensitivities.

Fig. 8 shows that the path-averaged sensitivities can be well predicted over space if having all data of P , E_0 , and R .

Fig. 9 shows the prediction performance in the absence of runoff data as it frequently occurs in practices.

13. [At Line 311-312 it is argued that the timing of precipitation change is important. I did not see this aspect in the results.]

Response: This sentence is problematic. I have removed it.

Reference

Zhou, S., B. Yu, L. Zhang, Y. Huang, M. Pan, and G. Wang (2016), A new method to partition climate and catchment effect on the mean annual runoff based on the Budyko complementary relationship. *Water Resources Research*, 52, 7163–7177. <https://doi.org/10.1002/2016WR019046>, 2016.

Ning, T., Li, Z., and W. Liu: Vegetation dynamics and climate seasonality jointly control the interannual catchment water balance in the Loess Plateau under the Budyko framework, *Hydrology and Earth System Sciences*, 21, 1515-1526. <https://doi.org/10.5194/hess-2016-484>, 2017.

1 | **A line integral-based and mathematically-precise method to partition climate**
2 | **and catchment effects on runoff**

3 | Mingguo Zheng^{1, 2*}

4 |
5 | ¹ Guangdong Key Laboratory of Agricultural Environment Pollution Integrated Control, Guangdong
6 | Institute of Eco-environment Science & Technology, Guangzhou 510650, China

7 | ² Key Laboratory of Water Cycle and Related Land Surface Processes, Institute of Geographic Sciences
8 | & Natural Resources Research, Chinese Academic of Sciences, Beijing 100101, China

9 | Correspondence: Mingguo Zheng (mgzheng@soil.gd.cn)

10 |
11 | **Abstract**

12 | It is a common task to partition synergistic impacts of a number of drivers in ~~the~~ environmental
13 | sciences. However, there is no mathematically precise solution to the partition. Here I presented a line
14 | integral-based method, which concerns about the sensitivity to the drivers throughout their evolutionary
15 | path so as to ensure a precise partition. The method reveals that the partition depends on both the
16 | change magnitude and pathway (timing of change), and not on the magnitude alone unless for a linear
17 | system. To illustrate the method, I used the Budyko framework to partition the effects on the temporal
18 | change in runoff of climatic and catchment conditions for 21 catchments from Australia and China. The
19 | method reduced to the decomposition method when assumed a path along which climate change occurs
20 | first followed by an abrupt change in catchment properties. The method re-defines the widely-used
21 | concept of sensitivity at a point as the path-averaged sensitivity. The total differential and the
22 | complementary methods simply concern about the sensitivity at the initial or/and the terminal state, so
23 | that they cannot give precise results. The path-average sensitivity of water yield to climate conditions
24 | was found to be stable over time. Space-wise, moreover, it can be readily predicted even in the absence
25 | of streamflow observations, whereby facilitates evaluation of future climate effects on streamflow. As a
26 | mathematically accurate solution, the method provides a generic tool to conduct the quantitative
27 | attribution analyses.

28 |
29 | **Keywords:** Runoff; Climate change; Human activities; Attribution analysis; Budyko

30 |
31 | **1 Introduction**

32 | It is often needed to quantify the relative roles of a few drivers to the observed changes of
33 | interest in ~~the~~ environmental sciences. In the hydrology community, diagnosing the relative
34 | contributions of climate change and human activities to runoff is of great relevance to the researchers
35 | and managers as both ~~of them climate change and human activities~~ have pose global-scale
36 | impact on hydrologic cycle and water resources (Barnett *et al.*, 2008; Xu *et al.*, 2014; Wang and Hejazi,
37 | 2001). ~~To date, u~~Unfortunately, the quantitative attribution analysis of the runoff changes remains a
38 | challenge (Wang and Hejazi, 2001; Berghuijs and Woods, 2016; Zhang *et al.*, 2016); this is to a

39 considerable degree due to a lack of a mathematically precise method to decouple synergistic and often
40 confounding impacts of climate change and human activities.

41 Numerous studies have detected the long term variability in runoff and attempted to partition the
42 effects of climate change and human activities by means of various methods (Dey and Mishra, 2017).
43 Among them are the paired-catchments method and the hydrological modeling method. The paired-
44 catchment method is believed to be able to filter the effect of climatic variability and thus isolate the
45 runoff change induced by vegetation changes (Brown *et al.*, 2005). However, the method is
46 capital intensive. Particularly, it generally involves small catchments and is challenged when
47 extrapolating to large catchments (Zhang *et al.*, 2011). The physical-based hydrological models often
48 suffer from limitations including high data requirement, labor-intensive calibration and validation
49 processes, and inherent uncertainty and interdependence in parameter estimations (Binley *et al.*, 1991;
50 Wang *et al.*, 2013; Liang *et al.*, 2015). Interest then turns to the conceptual models over recent years,
51 such as the Budyko-type equations (see Section 2.1).

52 Within the Budyko framework, a large number of studies (Roderick and Farquhar, 2011; Zhang
53 *et al.*, 2016) have used the total differential of runoff (i.e. dR , where R represents runoff) as a proxy for
54 the runoff change (i.e. ΔR) and further evaluated hydrological responses to climate change and human
55 activities (hereafter called the total differential method). ~~The total differential, however~~ However, dR is
56 essentially a first-order approximation of ΔR ~~the observed change~~ (Fig. 1(a)). It has been shown that the
57 approximation has caused an error of the climate impact on runoff ranging from 0 to 20 mm (or -118 to
58 174%) over China (Yang *et al.*, 2014). The total differential method directly used the partial derivatives
59 of runoff ~~to estimate~~ the sensitivities of runoff to climate and catchment conditions. Most studies
60 applied the forward approximation of the runoff change, i.e., using the sensitivities at the initial state
61 while calculation (e.g. Roderick and Farquhar, 2011). The elasticity method proposed by Schaake (1990)
62 is also based on the total differential expression (Sankarasubramanian *et al.*, 2001; Zheng *et al.*, 2009).
63 The method uses the “elasticity” concept to assess the climate sensitivity of runoff. The elasticity
64 coefficients, however, have been estimated in an empirical way and is not physically sound (Roderick
65 and Farquhar, 2011; Liang *et al.*, 2015).

66 The so-called decomposition method developed by Wang and Hejazi (2011) has also been
67 widely used. The method assumes that climate changes drive a shift along a Budyko curve and then
68 human interferences cause a vertical shift from the Budyko curve to another (Fig. 1(b)). Under this
69 assumption, the method ~~directly~~ extrapolates the Budyko models calibrated using observations of the
70 reference period, in which human impacts remain minimal, to determine the human-induced changes in
71 runoff occurred during the evaluation period.

72 Recently, Zhou *et al.* (2016) established a Budyko complementary relationship for runoff and
73 applied it to partitioning the climate and catchment effects. Superior to the total differential method, the
74 method culminates with yielding a no-residual partition. Nevertheless, the method depends on a given
75 weighted factor, which is determined in an empirical but not a precise way. Furthermore, Zhou *et al.*
76 (2016) argued that the partition is not unique in the Budyko framework as the path of the climate and
77 catchment changes cannot be uniquely identified.

78 ~~Actually, a~~ precise partition remains difficult even given a ~~a~~ precise mathematical model. This
79 can be illustrated by using a precise hydrology model $R = f(x, y)$, where R represents runoff, and x and y
80 climate factors and catchment characteristics respectively. We assumed that R changes by ΔR when x

带格式的: 字体: 倾斜

带格式的: 字体: 倾斜

域代码已更改

域代码已更改

81 changes by Δx and y by Δy , *i.e.* $\Delta R = f(x + \Delta x, y + \Delta y) - f(x, y)$. To determine the effect of x on ΔR ,
82 *i.e.* ΔR_x , a common practice is to assume that y remains constant when x changes by Δx . We thus get:
83 $\Delta R_x = f(x + \Delta x, y) - f(x, y)$. Similarly, we can get: $\Delta R_y = f(x, y + \Delta y) - f(x, y)$. Although the
84 derivation seems quite reasonable, it is problematic as the sum of ΔR_x and ΔR_y is not equal to ΔR .
85 Further examination shows that a variable's effect on R ~~seems to should~~ differ depending on the
86 changing path. For example, $\Delta R_x = f(x + \Delta x, y) - f(x, y)$ and $\Delta R_y = f(x + \Delta x, y + \Delta y) - f(x + \Delta x, y)$ if
87 x changes first and y subsequently (Note that the partition is precise with the sum of ΔR_x and ΔR_y
88 equals equaling ΔR now). If y changes first and x subsequently, ~~in contrast,~~ the expressions partition
89 then becomes: $\Delta R_x = f(x + \Delta x, y + \Delta y) - f(x, y + \Delta y)$ and $\Delta R_y = f(x, y + \Delta y) - f(x, y)$. In case of x
90 and y changing simultaneously, unfortunately, current literature seems not to provide a mathematically
91 precise solution.

92 The aims of this work are to propose a ~~new and~~ mathematically precise method to conduct
93 quantitative attribution to ~~the~~ drivers. The method is based on the line integer (called the LI method
94 hereafter) and takes account of the sensitivity throughout the evolutionary path of the drivers rather than
95 at a point as the the total differential does. In this way, thus the method revising-revises the widely-used
96 concept of sensitivity at a point as the path-averaged sensitivity. To present and evaluate the method, I
97 decomposed the relative influences of climate and catchment conditions on runoff within the Budyko
98 framework using data from 21 catchments from Australia and China. I also examined the spatio-
99 temporal variability of the path-averaged sensitivities of runoff to climatic and catchment conditions
100 and assessed their spatio-temporal predictability.

101

102 2 Methodology

103 2.1 The Budyko Framework and the MCY equation

104 Budyko (1974) argued that the mean annual evapotranspiration (E) is largely determined by
105 water and energy balance of a catchment. Using precipitation (P) and potential evapotranspiration (E_0)
106 as proxies for water and energy availabilities respectively, the Budyko framework
107 relates evapotranspiration losses to the aridity index defined as the ratio of E_0 over P . The Budyko
108 framework has gained wide acceptance in the hydrology community (Berghuijs and Woods, 2016;
109 Sposito, 2017). Over past decades, a number of equations have been developed to describe the
110 framework. Among them, the Mezentsev-Choudhury-Yang's equation (Mezentsev, 1955; Choudhury,
111 1999; Yang *et al.*, 2008) (Called the MCY equation hereafter) has been widely accepted and was used
112 here:

$$113 \frac{E}{P} = \frac{E_0/P}{(1 + (E_0/P)^n)^{1/n}} \quad (1)$$

114 where $n \in (0, \infty)$ is an integration constant that is dimensionless, and represents catchment properties.
115 Eq. (3) requires a relative long time scale whereby the water storage of a catchment is negligible and the
116 water balance equation reduces to be $R = P - E$; ~~where R denotes mean annual runoff~~. Here I adopted a

117 “tuned” n value that can get exact agreement between the calculated E by Eq. (1) and that actually
 118 encountered ($= P - R$).

119 The partial differentials of R with respect to P , E_0 , and n are given as:

$$120 \quad \frac{\partial R}{\partial P} = R_P(P, E_0, n) = 1 - \frac{E_0^{n+1}}{(P^n + E_0^n)^{1/n}} \quad (2a)$$

$$121 \quad \frac{\partial R}{\partial E_0} = R_{E_0}(P, E_0, n) = -\frac{P^{n+1}}{(P^n + E_0^n)^{1/n}} \quad (2b)$$

$$122 \quad \frac{\partial R}{\partial n} = R_n(P, E_0, n) = \frac{-E_0 P n^{-1}}{(P^n + E_0^n)^{1/n}} \left[\frac{\ln(P^n + E_0^n)}{n} - \frac{P^n \ln P + E_0^n \ln E_0}{P^n + E_0^n} \right] \quad (2c)$$

123 2.2 The theory of the line integral-based method

124 To present the LI method, we start by considering an example of a two-variable function $z = f(x,$
 125 $y)$, which has continuous partial derivatives $\partial z / \partial x = f_x(x, y)$ and $\partial z / \partial y = f_y(x, y)$. Suppose that x and y
 126 varies along a smooth curve L (e.g. AC in [Fig. 1\(c\)](#)) from the initial state (x_0, y_0) to the terminal
 127 state (x_N, y_N) , and z co-varies from z_0 to z_N . Let $\Delta z = z_N - z_0$, $\Delta x = x_N - x_0$, and $\Delta y = y_N - y_0$. Our goal is
 128 to seek for a mathematical solution to quantify the effects of Δx and Δy on Δz , i.e. Δz_x and Δz_y . Δz_x
 129 and Δz_y should be subject to the constraint $\Delta z_x + \Delta z_y = \Delta z$.

130 As shown in [Fig. 1\(c\)](#), points $M_1(x_1, y_1), \dots, M_{N-1}(x_{N-1}, y_{N-1})$ partition L into N distinct
 131 segments. Let $\Delta x_i = x_{i+1} - x_i$, $\Delta y_i = y_{i+1} - y_i$, and $\Delta z_i = z_{i+1} - z_i$. For each segment, Δz_i can be
 132 approximated as the total differential dz_i : $\Delta z_i \approx dz_i = f_x(x_i, y_i)\Delta x_i + f_y(x_i, y_i)\Delta y_i$. We then have:

$$133 \quad \Delta z = \sum_{i=1}^N \Delta z_i \approx \sum_{i=1}^N f_x(x_i, y_i)\Delta x_i + \sum_{i=1}^N f_y(x_i, y_i)\Delta y_i. \text{ We thus obtain an approximation of } \Delta z_x \text{ and } \Delta z_y :$$

$$134 \quad \Delta z_x \approx \sum_{i=1}^N f_x(x_i, y_i)\Delta x_i \text{ and } \Delta z_y \approx \sum_{i=1}^N f_y(x_i, y_i)\Delta y_i. \text{ Define } \tau \text{ as the maximum length among the } N \text{ segments.}$$

135 The smaller the value of τ , the closer to Δz_i the value of dz_i , and then the better the approximations are.

136 The approximations ~~would~~ becomes exact in the limit $\tau \rightarrow 0$. Taking the limit $\tau \rightarrow 0$ then turns sum
 137 into integrals and gives a precise expression (it is an informal derivation and please see Appendix A for

138 a formal one): $\Delta z = \lim_{\tau \rightarrow 0} \sum_{i=1}^N f_x(x_i, y_i)\Delta x_i + \lim_{\tau \rightarrow 0} \sum_{i=1}^N f_y(x_i, y_i)\Delta y_i = \int_L f_x(x, y)dx + \int_L f_y(x, y)dy$, where

$$139 \quad \int_L f_x(x, y)dx = \lim_{\tau \rightarrow 0} \sum_{i=1}^N f_x(x_i, y_i)\Delta x_i \text{ and } \int_L f_y(x, y)dy = \lim_{\tau \rightarrow 0} \sum_{i=1}^N f_y(x_i, y_i)\Delta y_i \text{ denote the line integral of } f_x \text{ and } f_y$$

140 along L (termed integral path) with respect to x and y , respectively. $\int_L f_x(x, y)dx$ and $\int_L f_y(x, y)dy$ exist

141 provided that f_x and f_y are continuous along L . We thus obtain a precise evaluation of Δz_x and Δz_y :

$$142 \quad \Delta z_x = \int_L f_x(x, y)dx \quad (3a)$$

$$143 \quad \Delta z_y = \int_L f_y(x, y)dy. \quad (3b)$$

144 [Unlike the total differential method](#) ~~Mathematically~~, the sum of Δz_x and Δz_y persistently equals
 145 Δz , ~~independent of the curve L~~ (Appendix B). If $f(x, y)$ is linear, then f_x and f_y are constant. Define
 146 $C_x = f_x(x, y)$ and $C_y = f_y(x, y)$, we have $\Delta z_x = C_x \Delta x$ and $\Delta z_y = C_y \Delta y$. Δz_x and Δz_y are thus independent of L .
 147 If $f(x, y)$ is non-linear, ~~in contrast~~ [however](#), both Δz_x and Δz_y varies with L , as was exemplified in
 148 Appendix C. Hence, the initial and the terminal states, together with the path connecting them,
 149 determines [the \$\Delta z_x\$ and \$\Delta z_y\$ unless resultant partition unless](#) $f(x, y)$ is linear.

150 The mathematical derivation above applies to a three-variable function as well. By doing the line
 151 integrals for the MCY equation, we obtain the desired results:

$$152 \quad \Delta R_P = \int_L \frac{\partial R}{\partial P} dP \quad (4a)$$

$$153 \quad \Delta R_{E_0} = \int_L \frac{\partial R}{\partial E_0} dE_0 \quad (4b)$$

$$154 \quad \Delta R_n = \int_L \frac{\partial R}{\partial n} dn \quad (4c)$$

155 where ΔR_P , ΔR_{E_0} , and ΔR_n denotes the effects on runoff change of P , E_0 , and n , respectively. The sum of
 156 ΔR_P and ΔR_{E_0} represents the effect of climate change, and ΔR_n are often related to human activities
 157 although it probably includes the effects of other factors, such as climate seasonality (Roderick and
 158 Farquhar, 2011; Berghuijs and Woods, 2016). L denotes a three-dimensional curve along which climate
 159 and catchment changes have occurred. I approximated L as a union of a series of line segments. ΔR_P ,
 160 ΔR_{E_0} , and ΔR_n were finally figured out by summing up the integrals along each of the line segments (see
 161 Section 2.3).

162 2.3 Using the LI method to determine ΔR_P , ΔR_{E_0} , and ΔR_n within the Budyko Framework

163 1) Determining ΔR_P , ΔR_{E_0} , and ΔR_n assuming a linear integral path

164 Given two consecutive periods and assumed that the catchment state has evolved from $(P_1, E_{01},$
 165 $n_1)$ to (P_2, E_{02}, n_2) along a straight line L . Let $\Delta P = P_2 - P_1$, $\Delta E_0 = E_{02} - E_{01}$, and $\Delta n = n_2 - n_1$, then the
 166 line L is given by ~~the~~ parametric equations: $P = \Delta P t + P_1$, $E_0 = \Delta E_0 t + E_{01}$, $n = \Delta n t + n_1$, $t \in [0, 1]$.
 167 Given the equations, Eq. (2) becomes a one-variable function of t , i.e., $\partial R / \partial P = R_P(t)$, $\partial R / \partial E_0 = R_{E_0}(t)$,
 168 and $\partial R / \partial n = R_n(t)$. Then, ΔR_P , ΔR_{E_0} , and ΔR_n can be evaluated as:

$$169 \quad \Delta R_P = \int_L \frac{\partial R}{\partial P} dP = \int_0^1 R_P(t) d(\Delta P t + P_1) = \Delta P \int_0^1 R_P(t) dt \quad (5a)$$

$$170 \quad \Delta R_{E_0} = \int_L \frac{\partial R}{\partial E_0} dE_0 = \int_0^1 R_{E_0}(t) d(\Delta E_0 t + E_{01}) = \Delta E_0 \int_0^1 R_{E_0}(t) dt \quad (5b)$$

$$171 \quad \Delta R_n = \int_L \frac{\partial R}{\partial n} dn = \int_0^1 R_n(t) d(\Delta n t + n_1) = \Delta n \int_0^1 R_n(t) dt \quad (5c)$$

172 Unfortunately, I cannot figure out the antiderivatives of $R_P(t)$, $R_{E_0}(t)$, and $R_n(t)$ and have to make
 173 approximate calculations. [As the discrete equivalent of integration is summation, we can approximate](#)
 174 [integration as summation.](#) I divided the $t \in [0, 1]$ interval into 1000 subintervals of the same width,
 175 thereby setting dt identically equal to 0.001, ~~and then~~ then calculated $R_P(t)dt$, $R_{E_0}(t)dt$, and $R_n(t)dt$ for

域代码已更改

带格式的: 字体: (默认) Times
New Roman, (中文) Calibri

176 each subinterval. Let $t_i = 0.001i, i \in [0, 999]$ and is integer-valued, $\Delta R_P, \Delta R_{E_0}$, and ΔR_n was approximated
 177 as:

$$178 \quad \Delta R_P \approx 0.001 \Delta P \sum_{i=0}^{999} R_P(t_i) \quad (6a)$$

$$179 \quad \Delta R_{E_0} \approx 0.001 \Delta E_0 \sum_{i=0}^{999} R_{E_0}(t_i) \quad (6b)$$

$$180 \quad \Delta R_n \approx 0.001 \Delta n \sum_{i=0}^{999} R_n(t_i) \quad (6c)$$

181 2) Dividing the evaluation period into a number of subperiods

182 I first determine a change point and divide the whole observation period into the reference and
 183 evaluation periods. To determine the integral path, the evaluation period is further divided into a
 184 number of subperiods. The Budyko framework assumes a steady state condition of a catchment and
 185 therefore requires no change in soil water storage. Over a time period of 5-10 years, it is reasonable to
 186 assume that changes in soil water storage are sufficiently small (Zhang *et al.*, 2001). Here I divided the
 187 evaluation period into a number of 7-year subperiods with the exception for the last one, which varied
 188 from 7 to 13 years in length depending on the length of the evaluation period.

189 3) Determining $\Delta R_P, \Delta R_{E_0}$, and ΔR_n by approximating the integral path as a series of line segments
 190 As did in Fig. 1(c), a curve can generally be approximated as a series of line segments. For
 191 a short period, the integral path L can be considered as linear, which implies a temporally invariant
 192 change rate/uniform change over time. For a long period, in which the change rate usually varies over
 193 time, if the change is not uniform over a given long period, the integral path L can be fitted using a
 194 number of line segments. Given a reference period and an evaluation period comprising N subperiods, I
 195 assumed that the catchment state evolved from $(P_0, E_{00}, n_0), \dots, (P_i, E_{0i}, n_i), \dots, (P_N, E_{0N}, n_N)$, where
 196 the subscript "0" denotes the reference period, and "i" and "N" denotes the i th and the last subperiods of
 197 the evaluation period, respectively. I used a series of line segments L_1, L_2, \dots, L_N to approximate the
 198 integral path L , where L_1 connects (P_0, E_{00}, n_0) with (P_1, E_{01}, n_1) , L_i connects points $(P_{i-1}, E_{0,i-1}, n_{i-1})$ with
 199 (P_i, E_{0i}, n_i) , and the initial point of L_{i+1} is the terminal point of L_i , and L_i connects points $(P_{i-1}, E_{0,i-1}, n_{i-1})$
 200 with (P_i, E_{0i}, n_i) and L_1 connects (P_0, E_{00}, n_0) with (P_1, E_{01}, n_1) . Then $\Delta R_P, \Delta R_{E_0}$, and ΔR_n are determined
 201 evaluated as the sum of the integrals along each of the line segments, which was calculated using Eq.
 202 (6).

203 2.4 The total-differential, decomposition and complementary methods

204 To evaluate the LI method, I compared it with the decomposition method, the total differential
 205 method, and the complementary method. The total differential method approximated ΔR as dR :

$$206 \quad \Delta R \approx dR = \frac{\partial R}{\partial P} \Delta P + \frac{\partial R}{\partial E_0} \Delta E_0 + \frac{\partial R}{\partial n} \Delta n = \lambda_P \Delta P + \lambda_{E_0} \Delta E_0 + \lambda_n \Delta n \quad (7)$$

207 where $\lambda_P = \partial R / \partial P$, $\lambda_{E_0} = \partial R / \partial E_0$, and $\lambda_n = \partial R / \partial n$, representing the sensitivity coefficient of R with
 208 respect to P, E_0 , and n , respectively. Within the total differential method, $\Delta R_P = \lambda_P \Delta P$, $\Delta R_{E_0} = \lambda_{E_0} \Delta E_0$, and
 209 $\Delta R_n = \lambda_n \Delta n$. I used a-the forward approximation, *i.e.* substituting the observed mean annual values of

the reference period into Eq. (2), to estimate λ_P , λ_{E_0} , and λ_n , as did in most studies (Roderick and Farquhar, 2011; Yang and Yang, 2011; Sun *et al.*, 2014).

The decomposition method (Wang and Hejazi, 2011) calculated ΔR_n as follows:

$$\Delta R_n = R_2 - R_2^i = (P_2 - E_2) - (P_2 - E_2^i) = E_2^i - E_2 \quad (8)$$

where R_2 , P_2 , and E_2 represents the mean annual runoff, precipitation and evapotranspiration of the evaluation period; and R_2^i and E_2^i represents the mean annual runoff and evapotranspiration respectively, given the climate conditions of the evaluation period and the catchment conditions of the reference period. Both E_2 and E_2^i were calculated by Eq. (1), but using n values of the evaluation period and the reference period respectively.

The complementary method (Zhou *et al.*, 2016) uses a linear combination of the complementary relationship for runoff to determine ΔR_P , ΔR_{E_0} , and ΔR_n :

$$\begin{aligned} \Delta R = a & \left[\left(\frac{\partial R}{\partial P} \right)_1 \Delta P + \left(\frac{\partial R}{\partial E_0} \right)_1 \Delta E_0 + P_2 \Delta \left(\frac{\partial R}{\partial P} \right) + E_{0,2} \Delta \left(\frac{\partial R}{\partial E_0} \right) \right] \\ & + (1-a) \left[\left(\frac{\partial R}{\partial P} \right)_2 \Delta P + \left(\frac{\partial R}{\partial E_0} \right)_2 \Delta E_0 + P_1 \Delta \left(\frac{\partial R}{\partial P} \right) + E_{0,1} \Delta \left(\frac{\partial R}{\partial E_0} \right) \right] \end{aligned} \quad (9)$$

where the subscript 1 and 2 denotes the reference and the evaluation periods, respectively. a is a weighting factor and varies from 0 to 1. As suggested by Zhou *et al.* (2016), I set $a = 0.5$. Equation (9) thus gave an estimation of ΔR_P , ΔR_{E_0} , and ΔR_n as follows:

$$\Delta R_P = 0.5 \Delta P \left[\left(\frac{\partial R}{\partial P} \right)_1 + \left(\frac{\partial R}{\partial P} \right)_2 \right] \quad (10a)$$

$$\Delta R_{E_0} = 0.5 \Delta E_0 \left[\left(\frac{\partial R}{\partial E_0} \right)_1 + \left(\frac{\partial R}{\partial E_0} \right)_2 \right] \quad (10b)$$

$$\Delta R_n = 0.5 \Delta \left(\frac{\partial R}{\partial P} \right) (P_1 + P_2) + 0.5 \Delta \left(\frac{\partial R}{\partial E_0} \right) (E_{0,1} + E_{0,2}) \quad (10c)$$

2.5 Data

I collected data of runoff and climate of 21 selected catchments from previous studies (Table 1). The change-point years gave in the studies was directly used to determine the reference and evaluation periods for the LI method. As mentioned above, the LI method further divides the evaluation period into a number of subperiods. For the sake of comparison, the last subperiod of the evaluation period was used as the evaluation period for the decomposition, the total differential and the complementary methods (It can be equally considered that all ~~of the four~~ methods used the last subperiod as the evaluation period, but the LI method cares about the intermediate period between the reference and the evaluation periods and the others do not). Nine of the 21 catchments had a reference period comprising only one subperiod (Table 1), and the others had two to seven.

The 21 selected catchments were located in diverse climates and landscapes. Among them, 14 are from Australia and 7 from China (Table 1). The catchments spanned from tropical to subtropical and temperate and from humid to semi-humid and semi-arid regions, with mean annual rainfall varying from 506 to 1014 mm and potential evaporation from 768 to 1169 mm. The index of dryness ranges

242 between 0.86 and 1.91. The catchment areas vary by five orders of magnitude from 1.95 to 121,972
 243 with a median 606 km². The key data includes annual runoff, precipitation, and potential evaporation.
 244 The record length varied between 15 and 75 with a median of 35 years. Among the 21 catchments, the
 245 changes from the reference to the evaluation period ranged between -271 and 79 mm yr⁻¹ for
 246 precipitation, and -35 and 41 mm yr⁻¹ for potential evaporation (Table 2). The coeval change in the
 247 parameter n of the MCY equation ranged between -0.2 to 2.53. All of the catchments experienced both
 248 climate change and land cover change over the observation period. The mean annual streamflow
 249 reduced for all of them, by from 0.43 to 229 with a median 38 mm yr⁻¹. More details of data and the
 250 catchments can be found in Zhang *et al.* (2011), Sun *et al.* (2014), Zhang *et al.* (2010), Zheng *et al.*
 251 (2009), Jiang *et al.* (2015), and Gao *et al.* (2016).
 252

253 3 Results

254 3.1 Comparisons with ~~other~~ ~~previous~~ ~~existing~~ methods

255 The LI method first partitions the whole observation period into the reference and evaluation
 256 periods, then further divides the latter into a number of subperiods and evaluates the contributions to
 257 runoff from climate and catchment changes for each subperiod, and finally adds up the derived
 258 contributions. Table 3 lists all of the resultant values of ΔR_P , ΔR_{E_0} , and ΔR_n of the LI method, together
 259 with the three other methods.

260 Fig. 2(a) compares the resultant ΔR_n of the LI method and the decomposition method. Although
 261 they are quite similar, the discrepancies between them can be up to >20 mm yr⁻¹. The decomposition
 262 method assumes that climate change occurs first and then human interferences cause a sudden change in
 263 catchment properties. Such a fictitious path is identical to the broken line AB+BC in ~~Fig. 1(c)~~,
 264 provided that x represents climate factors and y catchment properties. As a result, the decomposition
 265 method can be considered as a special case of the LI method when adopting the broken line AB+BC as
 266 the integral path, as was demonstrated clearly in Fig. 2(b).

267 The total differentiae method is predicated on an approximate equation, *i.e.* Eq. (7). The LI
 268 method reveals that the precise form of the equation is $\Delta R = \bar{\lambda}_P \Delta P + \bar{\lambda}_{E_0} \Delta E_0 + \bar{\lambda}_n \Delta n$ (*i.e.* Eq. (D2) in
 269 Appendix D), where $\bar{\lambda}_P$, $\bar{\lambda}_{E_0}$ and $\bar{\lambda}_n$ (Table 4) denote the path-averaged sensitivity of R to P , E_0 , and n ,
 270 respectively. All points along the path have the same weight in determining $\bar{\lambda}_P$, $\bar{\lambda}_{E_0}$ and $\bar{\lambda}_n$. To
 271 determine them, the total differential method utilizes only the initial state and the complementary
 272 method utilizes the initial and the terminal states. Neglecting the intermediate states between the initial
 273 and the terminal ones ~~even~~ possibly results in a reverse trend estimation (see ΔR_{E_0} for Catchment NO. 1
 274 in Table 3). Although the elasticity method exploits information contained over the entire observation
 275 period (*e.g.* Zheng *et al.*, 2009; Wang *et al.*, 2013), the resultant descriptive statistics of climate
 276 elasticity may not be robust (Roderick and Farquhar, 2011; Liang *et al.*, 2015).

277 Superior to the total differential method, the sum of ΔR_P , ΔR_{E_0} , and ΔR_n always equaled to ΔR
 278 for the LI method. ~~In addition, e~~ Examination of the subperiods ~~of the evaluation period~~ revealed that
 279 $\partial R / \partial n$ was more temporally variable than $\partial R / \partial P$ and $\partial R / \partial E_0$ (discussed below). For this reason, ΔR_n

280 showed considerable discrepancies between the two methods although ΔR_P as well as ΔR_{E_0} ~~was highly~~
281 ~~correlated~~ matched well between the two methods (Fig. 3).

282 As with the LI method, the complementary method produced ΔR_P , ΔR_{E_0} , and ΔR_n that exactly
283 add up to a ΔR on a par with the observed values. ~~The~~ Although ΔR_P , ΔR_{E_0} , and ΔR_n estimated by the
284 complementary method were all in good agreement with the LI method (Fig. 4). ~~However,~~ the LI
285 method often yielded values beyond the bounds given by the complementary method (Fig. 5); this is
286 because the initial and terminal states are not equivalent to the maximum and minimum values over the
287 integral path.

288 3.2 The spatio-temporal variability of the path-averaged sensitivities

289 $\bar{\lambda}_P$, $\bar{\lambda}_{E_0}$ and $\bar{\lambda}_n$ implies the average runoff change induced by a unit change in P , E_0 and n ,
290 respectively (Appendix D). Their spatio-temporal variability is relevant to the prediction of the runoff
291 change. To evaluate their temporal ~~variability~~ variabilities, I calculated $\bar{\lambda}_P$, $\bar{\lambda}_{E_0}$ and $\bar{\lambda}_n$ for each
292 subperiod of the evaluation period and assessed their deviation from those for the whole evaluation
293 period. As shown in Fig. 6, the deviation was rather limited for $\bar{\lambda}_P$ (averaged 8.6%) and $\bar{\lambda}_{E_0}$ (averaged
294 13%), but was considerable for $\bar{\lambda}_n$ (averaged 41%). Hence, it seems quite safe to predict the future
295 climate effects on runoff using earlier $\bar{\lambda}_P$ and $\bar{\lambda}_{E_0}$, but care must be taken when using earlier $\bar{\lambda}_n$ to
296 predict future catchment effect on runoff.

297 Different from the temporal variability, $\bar{\lambda}_P$, $\bar{\lambda}_{E_0}$ and $\bar{\lambda}_n$ all varied greatly, by up to several or
298 even ten folds, between the studied catchments (Table 4). It was found that there were good correlations
299 between $\bar{\lambda}_P$ and P , between $\bar{\lambda}_{E_0}$ and P , and between $\bar{\lambda}_n$ and n (Fig. 7). Fig. 8 shows that Eq. (2)
300 reproduced $\bar{\lambda}_P$, $\bar{\lambda}_{E_0}$ and $\bar{\lambda}_n$ very well taking the long-term means of P , E_0 , and n as inputs, a fact that the
301 dependent variable approached its average if setting the independent variables to be their averages. The
302 finding is of relevance to the spatial prediction of $\bar{\lambda}_P$, $\bar{\lambda}_{E_0}$, and $\bar{\lambda}_n$; moreover, it would greatly facilitate
303 the prediction of future climate effect on runoff as $\bar{\lambda}_P$ and $\bar{\lambda}_{E_0}$ was rather stable over time as previously
304 mentioned.

305 Runoff data and in turn, the parameter n in the MCY equation, are often unavailable. It is thus
306 desirable to make predictions of $\bar{\lambda}_P$, $\bar{\lambda}_{E_0}$ and $\bar{\lambda}_n$ in the absence of the parameter n . I developed three
307 strategies as follows: 1) using Eq. (2) and assuming $n = 2$ as n is typically in a small range from 1.5 to
308 2.6 (Roderick and Farquhar, 2011); 2) using P and E_0 to establish regression models; 3) using the aridity
309 index to establish regressions as it appeared to be more correlated with both $\bar{\lambda}_P$ and $\bar{\lambda}_{E_0}$ than P and E_0
310 (Fig. 7). As shown in Fig. 9, the three strategies have similar performance although the second one
311 seems to perform better. All of the strategies gave acceptable predictions of $\bar{\lambda}_P$ and $\bar{\lambda}_{E_0}$, but rather poor
312 results for $\bar{\lambda}_n$ as it was primarily controlled by n (Fig. 7). It was thus needed to seek more sophisticated
313 approaches to predict the future catchment effect on runoff in the absence of runoff observations.
314

域代码已更改

域代码已更改

域代码已更改

域代码已更改

域代码已更改

域代码已更改

315 **4 Discussion**

316 The LI method re-defines the widely-used concept of sensitivity at a point as the path-averaged
317 sensitivity. The LI method re-defines the widely used concept of sensitivity at a point as the path-
318 averaged sensitivity. The LI method highlights the role of the evolutionary path in determining the
319 resultant partition. Yet, it seems that no studies have taken into account the path issue when while
320 evaluating the relative influences of drivers. Compared with the existing methods, the limit of the
321 LI method is higher data requirement for obtaining the evolutionary path. When the data are unavailable,
322 the complementary method can be considered as an alternative. First, the method offer results
323 free of residuals; in addition, it employs both data of the reference and the evaluation periods to
324 determine the sensitivities, thus generally yielding values closer to the path-averaged sensitivities than
325 the total differentiae method.

326 While using the Budyko models, a reasonable time scale is relevant to meet the assumption that
327 changes in catchment water storage are small relative to the magnitude of fluxes of P , R and E . The
328 present study selected seven years as most studies have suggested a time period of 5-10 years (Zhang et
329 al., 2001; Zhang et al., 2016; Wu et al., 2017a; Wu et al., 2017b; Li et al., 2017), or even one year
330 (Roderick and Farquhar, 2011; Sivapalan et al., 2011; Carmona et al., 2014; Ning et al., 2017).
331 Nevertheless, some studies argue that the time period should be longer than ten years (Li et al., 2016;
332 Dey and Mishra, 2017). If this is the case, the high temporal variation of λ_n shown in Fig. 6 might be
333 caused by water storage changes, rather than actual changes in the catchment properties. The
334 uncertainty should be addressed. Using the Gravity Recovery and Climate
335 Experiment (GRACE) satellite gravimetry, Zhao et al.(2011) detected the water storage variations for
336 three largest river basins of China, namely, Yellow, Yangtze, and Zhujiang. The Yellow River mostly
337 drains an arid and semiarid region (P , 450mm; R , 70 mm; E , 380mm), and the Yangtze (P , 110mm; R ,
338 550 mm; E , 550mm) and the Zhujiang river basins (P , 1400mm; R , 780 mm; E , 620mm) are humid. 黄河 P
339 来自“黄河流域干旱时空演变的空间格局研究”R 来自刘晓燕专著, 长江来自 2018 年水资源公报, 珠江根据水资源公报数据计算。 The amplitude of the
340 water storage variations between years were 7, 37.2 and 65 mm for the three rivers respectively, one
341 magnitude order smaller than fluxes of P , R and E . Although the observations cannot be directly
342 extrapolated to other regions, the possibility seems remote that the use of a 7-year aggregated time
343 strongly violate the assumption of the steady state condition.

345 In dry areas, the carryover of soil water storage between years is relatively small as much of the
346 annual precipitation is evaporated and thus has little effect in altering water storage. In the Yellow River
347 basin, most of which are arid or semi-arid, the Gravity Recovery and Climate
348 Experiment (GRACE) satellite gravimetry shows that the water storage variations between years (<7
349 mm) was negligible relative to the annual precipitation (450mm), so that the Budyko model can work at
350 a time scale of one year (Ning et al., 2017). Hence, the 7-year time scale should be at least appropriate for dry
351 catchments. We examined five driest catchments (aridity index >1.5) among the 21 catchments we used,
352 finding that λ_n remains to exhibit greater temporal variations than λ_P and λ_{E_0} for most of the
353 subperiods. The observation reinforced conclusions drawn from all of the catchments.未用, 可删
354 除。

带格式的: 字体: (默认) Times New Roman, 小四, 字体颜色: 黑色, (中文) 中文(中国), 图案: 清除

带格式的: 两端对齐, 缩进: 首行缩进: 2.95 字符, 定义网格后自动调整右缩进, 孤行控制, 调整中文与西文文字的间距, 调整中文与数字的间距

带格式的

域代码已更改

带格式的

带格式的

带格式的: 突出显示

域代码已更改

带格式的

域代码已更改

355
356
357
358
359
360
361
362
363
364
365
366
367
368
369
370
371
372
373
374
375

376
377
378
379
380
381
382
383
384
385
386

387

a more rigorous approach would be needed to settle that point, but reversal of the results obtained for the two-class seems a very remote possibility. It assumes that the carryover of water storage between years is negligible compared to the annual fluxes of P, E, and Q. Changes in catchment storage are small relative to the magnitude of fluxes (P, E, Q). This is a common assumption in annual water balance studies [Milly, 1994; Zhang et al., 2001; Yang et al., 2008; Sivapalan et al., 2011]; however, it is clearly not appropriate for smaller time scales since soil water storage variations at these temporal scales cannot be neglected [Cheng et al., 2011]. Nevertheless, to minimize the errors that can be introduced by this assumption, the Budyko framework assumes a steady state condition of a catchment and therefore requires no change in soil water storage. Over a time period of 5-10 years, it is reasonable to assume that changes in soil water storage are sufficiently small (Zhang et al., 2001). 可删除

~~It has been a great concern for hydrologist, agricultural scientist, geoscientist, catchment managers and others for more than 50 years that how much runoff change a 10% or 20% change in precipitation would result in (Roderick and Farquhar, 2011; Yang et al., 2014). The LI method reveals that the answer to the question varies with both the timing and magnitude of the precipitation change, not on the magnitude alone. Berghuijs and Woods (2016) claimed an asymmetry between spatial and temporal partitioning of precipitation into streamflow and evaporation. Unfortunately, they did not take account of the difference between the evolutionary paths over space and time, which also play a role in determining the resultant partitioning.~~

Mathematically, the LI method is unrelated to a functional form and applies to communities other than just hydrology. For example, identifying the carbon emission budgets (an allowable amount of anthropogenic CO₂ emission consistent with a limiting warming target), is crucial for global efforts to mitigate climate change. The LI method suggested that 1) the emission budgets depends on both the emission magnitude and pathway (timing of emissions), in line with a recent study by Gasser et al. (2018), and 2) an optimal pathway would bring about an elevated carbon budget unless the carbon-climate system behaves in a linear fashion. Their study presented the LI method using time-series data, but it The LI method applies equally to the case of spatial series of data. Given a model that relates fluvial or aeolian sediment load to the influencing factors (e.g. rainfall and topography), for example, the LI method can be used to separate the contributions of the factors to the sediment-load change along a river or in the along-wind direction

5 Conclusions

Based on the line integral, I found a mathematically precise solution to partition the effects of a number of independent variables on the change in the dependent variable. I then applied the method to partition the effects on runoff of climatic and catchment conditions within the Budyko framework. The method reveals that in addition to the change magnitude, the change pathways of climatic and catchment conditions also exert control on their impacts on runoff. Instead of using the runoff sensitivity at a point, the LI method uses the path-averaged sensitivity, thereby ensuring a mathematically precise partition. I further examined the spatiotemporal variability of the path-averaged

带格式的：突出显示

带格式的：左，缩进：首行缩进：0 字符，定义网格后不调整右缩进，无孤行控制，不调整西文与中文之间的空格，不调整中文和数字之间的空格

带格式的：左，缩进：首行缩进：0 字符，定义网格后不调整右缩进，无孤行控制，不调整西文与中文之间的空格，不调整中文和数字之间的空格

396 sensitivity. Time-wise the runoff sensitivity is stable to climate but highly variable to catchment
 397 properties, suggesting that it is reliable to predict future climate effects using earlier observations but
 398 care must be taken when predicting the catchment effects. Space-wise (between catchments) the runoff
 399 sensitivity was highly variable both to climatic and catchment conditions, but it can be well depicted by
 400 the long-term means of the climatic and catchment conditions. As a mathematically accurate scheme,
 401 the LI method has the potential to be a generic attribution approach in the environmental sciences.
 402

403 **Data availability**

404 The data used in this study are freely available by contacting the authors.
 405

406 **Author contribution**

407 MZ designed the study, analysing the data and wrote the manuscript.
 408

409 **Competing interests**

410 The authors declare that they have no conflict of interest.
 411

412 **Appendix A: Derivation of equation** $\Delta z = \int_L f_x(x, y)dx + \int_L f_y(x, y)dy$

413 We define that the curve L in ~~Fig. 1~~**Fig. 1(c)** is given by a parametric equation: $x = x(t)$, $y = y(t)$,
 414 $t \in [t_0, t_N]$, then $\Delta z = z_N - z_0 = f[x(t_N), y(t_N)] - f[x(t_0), y(t_0)]$. Substituting the parametric equations, we
 415 get:

416 The right-hand side of the equation = $\int_{t_0}^{t_N} f_x[x(t), y(t)]dx(t) + \int_{t_0}^{t_N} f_y[x(t), y(t)]dy(t)$

$$417 = \int_{t_0}^{t_N} \{ f_x[x(t), y(t)]x'(t) + f_y[x(t), y(t)]y'(t) \} dt \quad (A1)$$

418 Let $g(t) = f[x(t), y(t)]$, and after using the chain rule to differentiate g with respect to t , we obtain:

$$419 g'(t) = \frac{\partial g}{\partial x} \frac{dx}{dt} + \frac{\partial g}{\partial y} \frac{dy}{dt} = f_x[x(t), y(t)]x'(t) + f_y[x(t), y(t)]y'(t) \quad (A2)$$

420 It shows that $g'(t)$ is just the integrand in Eq. (A1), Eq. (A1) can then be rewritten as:

$$421 \text{The right-hand side of the equation} = \int_{t_0}^{t_N} g'(t) dt = [g(t)]_{t_0}^{t_N} = g(t_N) - g(t_0)$$

422 = $f[x(t_N), y(t_N)] - f[x(t_0), y(t_0)]$ = The left-hand side of the equation

423 **Appendix B: The sum of $\int_L f_x(x, y)dx$ and $\int_L f_y(x, y)dy$ is path independent**

424 **Theorem:** Given an open simply-connected region G (i.e., no holes in G) and two functions $P(x, y)$
 425 and $Q(x, y)$ that have continuous first-order derivatives, if and only if $\partial P / \partial y = \partial Q / \partial x$ throughout G ,

426 then $\int_L P(x, y)dx + \int_L Q(x, y)dy$ is path independent, i.e., it depends solely on the starting and ending
 427 point of L .

428 We have $\partial f_x / \partial y = \partial^2 z / \partial x \partial y$ and $\partial f_y / \partial x = \partial^2 z / \partial y \partial x$. As $\partial^2 z / \partial x \partial y = \partial^2 z / \partial y \partial x$, we can state that
 429 $\partial f_x / \partial y = \partial f_y / \partial x$, meeting the above condition and proving that $\int_L f_x(x, y)dx + \int_L f_y(x, y)dy$ is path
 430 independent. The statement was further exemplified using a fictitious example in Appendix C.

431 **Appendix C. A fictitious example to show how the LI method works**

432 It is assumed that runoff (R , mm yr⁻¹) at a site increases from 120 to 195 mm yr⁻¹ with $\Delta R = 75$ mm
 433 yr⁻¹; meanwhile, precipitation (P , mm yr⁻¹) varies from 600 to 650 mm yr⁻¹ ($\Delta P = 75$ mm yr⁻¹) and
 434 runoff coefficient (C_R , dimensionless) from 0.2 to 0.3 ($\Delta C_R = 0.1$). The goal is to partition ΔR into the
 435 effects of precipitation (ΔR_P) and runoff coefficient (ΔR_{C_R}) provided that P and C_R are independent.
 436 We have a function $R = PC_R$ and its partial derivatives $\partial R / \partial P = C_R$ and $\partial R / \partial C_R = P$. Given a path L
 437 along which P and C_R change and using Eq. (3), the LI method evaluates ΔR_P and ΔR_{C_R} as:

$$438 \quad \Delta R_{C_R} = \int_L \partial R / \partial C_R dC_R = \int_L P dC_R \quad \text{and} \quad \Delta R_P = \int_L \partial R / \partial P dP = \int_L C_R dP \quad (C1)$$

439 The result differs depending on L but the sum of ΔR_P and ΔR_{C_R} uniformly equals ΔR . It will be
 440 demonstrated using [Fig. 1\(c\)](#), in which the x -axis represents C_R and the y -axis P . Point A denotes
 441 the initial state ($C_R = 0.2, P = 600$) and point C the terminal state ($C_R = 0.3, P = 650$). I calculated ΔR_P
 442 and ΔR_{C_R} along three fictitious paths as follows:

443 1) $L=AC$. Line segment AC has equation $P = 500C_R + 500, 0.2 \leq C_R \leq 0.3$. Let's take C_R as the
 444 parameter and write the equation in the parametric form as $P = 500C_R + 500, C_R = C_R, 0.2 \leq C_R \leq 0.3$.
 445 By substituting the equation into Eq. (C1), we have:

$$446 \quad \Delta R_{C_R} = \int_{AC} P dC_R = \int_{0.2}^{0.3} (500C_R + 500) dC_R = 62.5$$

$$447 \quad \Delta R_P = \int_{AC} C_R dP = \int_{AC} C_R d(500C_R + 500) = 500 \int_{0.2}^{0.3} C_R dC_R = 12.5$$

448 2) $L=AB+BC$. To evaluate on the broken line, we can evaluate separately on AB and BC and then sum
 449 them up. The equation for AB is $P = 600, 0.2 \leq C_R \leq 0.3$, and is $C_R = 0.3, 600 \leq P \leq 650$ for BC.
 450 Notes that a constant C_R or P implies that $dC_R = 0$ or $dP = 0$. Eq. (C1) then becomes:

$$451 \quad \Delta R_{C_R} = \int_{AB+BC} P dC_R = \int_{AB} P dC_R + \int_{BC} P dC_R = \int_{0.2}^{0.3} 600 dC_R + 0 = 60$$

$$452 \quad \Delta R_P = \int_{AB+BC} C_R dP = \int_{AB} C_R dP + \int_{BC} C_R dP = 0 + \int_{600}^{650} 0.3 dP = 15$$

453 3) $L=AD+DC$. The equation for AD is $C_R = 0.2, 600 \leq P \leq 650$ and is $P = 650, 0.2 \leq C_R \leq 0.3$ for
 454 DC. ΔR_P and ΔR_{C_R} are evaluated as:

$$455 \quad \Delta R_{C_R} = \int_{AD+DC} P dC_R = \int_{AD} P dC_R + \int_{DC} P dC_R = 0 + \int_{0.2}^{0.3} 650 dC_R = 65$$

456
$$\Delta R_P = \int_{AD+DC} C_{rd}P = \int_{AD} C_{rd}P + \int_{DC} C_{rd}P = \int_{600}^{650} 0.2dP + 0 = 10$$

457 As we expected, the sum of ΔR_P and ΔR_{CR} persistently equals ΔR although ΔR_P and ΔR_{CR} varies with
 458 L .
 459

460 **Appendix D: Derivation of $\Delta R = \overline{\lambda_P}\Delta P + \overline{\lambda_{E_0}}\Delta E_0 + \overline{\lambda_n}\Delta n$**

461 If we partition the interval $[x_0, x_N]$ in **Fig. 1(c)** into N distinct bins of the same width
 462 $\Delta x_i = \Delta x/N$. Eq. (3a) can then be rewritten as:

463
$$\Delta Z_x = \int_L f_x(x, y)dx = \lim_{\tau \rightarrow 0} \sum_{i=0}^{N-1} f_x(x_i, y_i)\Delta x_i = \lim_{\tau \rightarrow 0} N \Delta x_i \frac{\sum_{i=0}^{N-1} f_x(x_i, y_i)}{N} = \Delta x \lim_{\tau \rightarrow 0} \frac{\sum_{i=0}^{N-1} f_x(x_i, y_i)}{N} = \overline{\lambda_x} \Delta x$$

464 where $\overline{\lambda_x} = \lim_{\tau \rightarrow 0} \frac{\sum_{i=1}^N f_x(x_i, y_i)}{N}$, denoting the average of $f_x(x, y)$ along the curve L . Likewise, we have

465 $\Delta Z_y = \overline{\lambda_y} \Delta y$, where $\overline{\lambda_y}$ denotes the average of $f_y(x, y)$ along the curve L . As a result, we have:

466
$$\Delta Z = \overline{\lambda_x} \Delta x + \overline{\lambda_y} \Delta y \quad (D1)$$

467 The result can readily be extended to a function of three variables. Applying the mathematic
 468 derivation above to the MCY Equation results in a precise form of Eq. (7):

469
$$\Delta R = \Delta R_P + \Delta R_{E_0} + \Delta R_n = \overline{\lambda_P}\Delta P + \overline{\lambda_{E_0}}\Delta E_0 + \overline{\lambda_n}\Delta n, \quad (D2)$$

470 where $\Delta R_P = \overline{\lambda_P}\Delta P$, $\Delta R_{E_0} = \overline{\lambda_{E_0}}\Delta E_0$, $\Delta R_n = \overline{\lambda_n}\Delta n$, and $\overline{\lambda_P}$, $\overline{\lambda_{E_0}}$ and $\overline{\lambda_n}$ denote the arithmetic mean of $\partial R/\partial P$,
 471 $\partial R/\partial E_0$, and $\partial R/\partial n$ along a path of climate and catchment changes, respectively. Because $\overline{\lambda_P} = \Delta R_P / \Delta P$,
 472 $\overline{\lambda_{E_0}} = \Delta R_{E_0} / \Delta E_0$, and $\overline{\lambda_n} = \Delta R_n / \Delta n$, $\overline{\lambda_P}$, $\overline{\lambda_{E_0}}$ and $\overline{\lambda_n}$ also implies the runoff change due to a unit change in
 473 P , E_0 and n , respectively.
 474

475 **Acknowledgments**

476 This work was funded by the National Natural Science Foundation of China (41671278), the GDAS'
 477 Project of Science and Technology Development (2019GDASYL-0103043) and (2019GDASYL-
 478 0502004). I thank Mr. Y.Q. Zheng for his assistance with the mathematic derivations.

480 **References**

481 Barnett, T. P., Pierce, D. W., Hidalgo, H. G., Bonfils, C., Santer, B. D., Das, T., Bala G., Woods, A. W.,
 482 Nozawa, T., Mirin, A. A., Cayan D. R., and M. D. Dettinger: Human-induced changes in the
 483 hydrology of the western United States. *Science*, 319(5866), 1080-1083.
 484 <https://doi.org/10.1126/science.1152538>, 2008.
 485 Berghuijs, W. R., R. A. Woods: Correspondence: Space-time asymmetry undermines water yield

486 assessment. *Nature Communications* 7, 11603. [https://doi.org/ 10.1038/ncomms11603](https://doi.org/10.1038/ncomms11603), 2016.

487 Binley, A. M., Beven, K. J., Calver, A., and L. G. Watts: Changing responses in hydrology: assessing
488 the uncertainty in physically based model predictions. *Water Resources Research*, 27(6), 1253-1261.
489 <https://doi.org/10.1029/91WR00130>, 1991.

490 Brown, A. E., Zhang, L., McMahon, T. A., Western, A. W. and R. A. Vertessy: A review of paired
491 catchment studies for determining changes in water yield resulting from alterations in vegetation.
492 *Journal of Hydrology*, 310, 26–61. [https://doi.org/ 10.1016/j.jhydrol.2004.12.010](https://doi.org/10.1016/j.jhydrol.2004.12.010), 2005.

493 Budyko, M. I.: *Climate and Life*. Academic, N. Y. 1974.

494 Carmona, A. M., Sivapalan, M., Yaeger, M. A., and Poveda, G.: Regional patterns of interannual
495 variability of catchment water balances across the continental US: A Budyko framework. *Water*
496 *Resources Research*, 50, 9177–9193. [https://doi:10.1002/2014wr016013](https://doi.org/10.1002/2014wr016013), 2014.

497 Choudhury, B. J.: Evaluation of an empirical equation for annual evaporation using field observations
498 and results from a biophysical model. *Journal of Hydrology*, 216, 99–110.
499 [https://doi.org/10.1016/S0022-1694\(98\)00293-5](https://doi.org/10.1016/S0022-1694(98)00293-5), 1999.

500 Dey, P., and A. Mishra: Separating the impacts of climate change and human activities on streamflow:
501 A review of methodologies and critical assumptions. *Journal of Hydrology*, 548, 278-290.
502 <https://doi.org/10.1016/j.jhydrol.2017.03.014>, 2017.

503 Gao, G., Ma, Y., and B. Fu: Multi-temporal scale changes of streamflow and sediment load in a loess
504 hilly watershed of China. *Hydrological Processes*, 30(3), 365-382, [10.1002/hyp.10585](https://doi.org/10.1002/hyp.10585), 2016.

505 Gasser, T., M. Kechiar, P. Ciais, E. J. Burke, T. Kleinen, D. Zhu, Y. Huang, A. Ekici, and M.
506 Obersteiner: Path-dependent reductions in CO₂ emission budgets caused by permafrost carbon
507 release. *Nature Geoscience*, 11, 830–835. [https://doi.org/ 10.1038/s41561-018-0227-0](https://doi.org/10.1038/s41561-018-0227-0), 2018.

508 Jiang, C., Xiong, L., Wang, D., Liu, P., Guo, S., and Xu C.: Separating the impacts of climate change
509 and human activities on runoff using the Budyko-type equations with time-varying parameters.
510 *Journal of Hydrology*, 522, 326-338, [10.1016/j.jhydrol.2014.12.060](https://doi.org/10.1016/j.jhydrol.2014.12.060), 2015.

511 Li, Z., Ning, T., Li, J., and D. Yang: Spatiotemporal variation in the attribution of streamflow changes
512 in a catchment on China's Loess Plateau. *Catena*, 158:1–8.
513 <https://doi.org/10.1016/j.catena.2017.06.008>, 2017.

514 Liang, W., D. Bai, F. Wang, B. Fu, J. Yan, S. Wang, Y. Yang, D. Long, and M. Feng: Quantifying the
515 impacts of climate change and ecological restoration on streamflow changes based on a Budyko
516 hydrological model in China's Loess Plateau. *Water Resources Research*, 51, 6500–6519.
517 <https://doi.org/10.1002/2014WR016589>, 2015.

518 Liu, J., Zhang, Q., Singh, V. P., and P. Shi: Contribution of multiple climatic variables and human
519 activities to streamflow changes across China. *Journal of Hydrology*, 545, 145-162.
520 <https://doi.org/10.1016/j.jhydrol.2016.12.016>, 2016.

521 Mezentsev, V. S.: More on the calculation of average total evaporation. *Meteorol. Gidrol.*, 5, 24–26,
522 1955.

523 Ning, T., Li, Z., and W. Liu: Vegetation dynamics and climate seasonality jointly control the
524 interannual catchment water balance in the Loess Plateau under the Budyko framework,
525 *Hydrology and Earth System Sciences*, 21, 1515-1526. <https://doi.org/10.5194/hess-2016-484>, 2017.

526 Roderick, M. L., and G. D. Farquhar: A simple framework for relating variations in runoff to variations
527 in climatic conditions and catchment properties. *Water Resources Research*, 47, W00G07,

528 <https://doi.org/10.1029/2010WR009826>, 2011.

529 Sankarasubramanian, A., R. M. Vogel, and J. F. Limbrunner: Climate elasticity of streamflow in the
530 United States. *Water Resources Research*, 37(6), 1771-1781.
531 <https://doi.org/10.1029/2000WR900330>, 2001.

532 Schaake, J. C.: From climate to flow. *Climate Change and U.S. Water Resources*, edited by P. E.
533 Waggoner, chap. 8, pp. 177 – 206, John Wiley, N. Y. 1990.

534 Sivapalan, M., Yaeger, M. A., Harman, C. J., Xu, X. Y., and P. A. Troch: Functional model of water
535 balance variability at the catchment scale: 1. Evidence of hydrologic similarity and space-time
536 symmetry, *Water Resources Research*, 47, W02522, doi:10.1029/2010wr009568, 2011.

537 Spósito, G.: Understanding the Budyko equation. *Water*, 9(4), 236. <https://doi.org/10.3390/w9040236>,
538 2017.

539 Sun, Y., Tian, F., Yang, L., and H. Hu: Exploring the spatial variability of contributions from climate
540 variation and change in catchment properties to streamflow decrease in a mesoscale basin by three
541 different methods. *Journal of Hydrology*, 508(2), 170-180,
542 <https://doi.org/10.1016/j.jhydrol.2013.11.004>, 2014.

543 Wang, D., and M. Hejazi: Quantifying the relative contribution of the climate and direct human impacts
544 on mean annual streamflow in the contiguous United States. *Water Resources Research*, 47, W00J12,
545 <https://doi.org/10.1029/2010WR010283>, 2011.

546 Wang, W., Q. Shao, T. Yang, S. Peng, W. Xing, F. Sun, and Y. Luo: Quantitative assessment of the
547 impact of climate variability and human activities on runoff changes: A case study in four
548 catchments of the Haihe River basin, China. *Hydrological Processes*, 27(8), 1158–1174.
549 <https://doi.org/10.1002/hyp.9299>, 2013.

550 Wu, J., Miao, C., Wang, Y., Duan, Q., and X. Zhang: Contribution analysis of the long-term changes in
551 seasonal runoff on the Loess Plateau, China, using eight Budyko-based methods. *Journal of*
552 *hydrology*, 545, 263-275. <https://doi.org/10.1016/j.jhydrol.2016.12.050>, 2017a.

553 Wu, J., Miao, C., Zhang, X., Yang, T., and Q. Duan: Detecting the quantitative hydrological response to
554 changes in climate and human activities. *Science of the Total Environment*, 586, 328-337.
555 <https://doi.org/10.1016/j.scitotenv.2017.02.010>, 2017b.

556 Xu, X., Yang, D., Yang, H. and Lei, H.: Attribution analysis based on the Budyko hypothesis for
557 detecting the dominant cause of runoff decline in Haihe basin. *Journal of Hydrology*, 510: 530-540.
558 <http://dx.doi.org/10.1016/j.jhydrol.2013.12.052>, 2014.

559 Yang, H., D. Yang, Z. Lei, and F. Sun: New analytical derivation of the mean annual water-energy
560 balance equation. *Water Resources Research*, 44, W03410. <https://doi.org/10.1029/2007WR006135>,
561 2008.

562 Yang, H., and D. Yang: Derivation of climate elasticity of runoff to assess the effects of climate change
563 on annual runoff. *Water Resources Research*, 47, W07526. <https://doi.org/10.1029/2010WR009287>,
564 2011.

565 Yang, H., D. Yang, and Q. Hu: An error analysis of the Budyko hypothesis for assessing the
566 contribution of climate change to runoff. *Water Resources Research*, 50, 9620–9629.
567 <https://doi.org/10.1002/2014WR015451>, 2014.

568 Zhao, Q. L., Liu, X. L., Ditmar, P., Siemes, C., Revtova, E., Hashemi-Farahani, H., and R. Klees: Water
569 storage variations of the Yangtze, Yellow, and Zhujiang river basins derived from the DEOS Mass

570 Transport (DMT-1) model. *Science China-Earth Sciences*, 54, 667-677.
571 <https://doi.org/10.1007/s11430-010-4096-7>, 2011.

572 Zhang, S., H. Yang, D. Yang, and A. W. Jayawardena: Quantifying the effect of vegetation change on
573 the regional water balance within the Budyko framework. *Geophysical Research Letters*, 43, 1140–
574 1148. <https://doi.org/10.1002/2015GL066952>, 2016.

575 Zhang, L., Dawes, W. R. and G. R. Walker: Response of mean annual evapotranspiration to vegetation
576 changes at catchment scale. *Water Resources Research* 37, 701–708. doi; 10.1029/2000WR900325,
577 2001.

578 Zhang, L., F. Zhao, A. Brown, Y. Chen, A. Davidson, and R. Dixon: Estimating Impact of Plantation
579 Expansions on Streamflow Regime and Water Allocation. CSIRO Water for a Healthy Country,
580 Canberra, Australia. 2010.

581 Zhang, L., F. Zhao, Y. Chen, and R. N. M. Dixon: Estimating effects of plantation expansion and
582 climate variability on streamflow for catchments in Australia. *Water Resources Research*, 47,
583 W12539, <https://doi.org/10.1029/2011WR010711>, 2011.

584 Zheng, H., L. Zhang, R. Zhu, C. Liu, Y. Sato, and Y. Fukushima: Responses of streamflow to climate
585 and land surface change in the headwaters of the Yellow River Basin. *Water Resources Research*, 45,
586 W00A19. <https://doi.org/10.1029/2007WR006665>, 2009.

587 Zhou, S., B. Yu, L. Zhang, Y. Huang, M. Pan, and G. Wang (2016), A new method to partition climate
588 and catchment effect on the mean annual runoff based on the Budyko complementary relationship.
589 *Water Resources Research*, 52, 7163–7177. <https://doi.org/10.1002/2016WR019046>, 2016.

590
591
592
593
594
595
596
597
598
599
600
601
602
603
604
605
606
607
608
609
610
611
612
613
614
615

Table 1. Summary of the long-term hydrometeorological characteristics of the selected catchments^a

Catchment No. ^b	Area (km ²)	<i>R</i>	<i>P</i>	<i>E</i> ₀	<i>n</i>	<i>AI</i>	Reference Period	Evaluation Period	The Last Subperiod
1	391	218	1014	935	3.5	0.92	1933-1955	1956-2008	1998-2008
2	16.64	32.9	634	1087	3.16	1.71	1979-1984	1985-2008	1999-2008
3	559	183	787	780	2.68	0.99	1960-1978	1979-2000	1993-2000
4	606	73	729	998	3.07	1.37	1971-1995	1996-2009	2003-2009
5	760	77.9	689	997	2.66	1.45	1970-1995	1996-2009	2003-2009
6	502	57.2	730	988	3.59	1.35	1974-1995	1996-2008	1996-2008
7	673	431	1013	953	1.34	0.94	1947-1955	1956-2008	1998-2008
8	390	139	840	1021	2.61	1.22	1966-1980	1981-2005	1995-2005
9	1130	20.7	633	1077	3.79	1.7	1972-1982	1983-2007	1997-2007
10	3.2	37.5	631	954	3.49	1.51	1989-1991	1992-2009	1999-2009
11	1.95	111	767	901	3.06	1.18	1990-1992	1993-2005	1993-2005
12	89	272	963	826	2.82	0.86	1958-1965	1966-1999	1987-1999
13	243	38.5	735	1010	4.27	1.37	1989-1995	1996-2007	1996-2007
14	56.35	65.8	744	1007	3.35	1.35	1989-1995	1996-2008	1996-2008
15	14484	385	893	1022	1.11	1.14	1970-1989	1990-2000	1990-2000
16	38625	461	985	1087	1.03	1.1	1970-1989	1990-2000	1990-2000
17	59115	388	897	1161	1.02	1.29	1970-1989	1990-2000	1990-2000
18	95217	371	881	1169	1.03	1.33	1970-1989	1990-2000	1990-2000
19	121,972	171	507	768	1.17	1.52	1960-1990	1991-2000	1991-2000
20	106,500	60.5	535	905	2.25	1.69	1960-1970	1971-2009	1999-2009
21	5891	34.4	506	964	2.54	1.91	1952-1996	1997-2011	2004-2011

^a*R*, *P*, and *E*₀ represents mean annual runoff, precipitation and potential evaporation, all in mm yr⁻¹. *n* (dimensionless) is the parameter representing catchment properties in the MCY equation. *AI* is dimensionless aridity index ($AI = E_0/P$). Data of Catchments 1-14 were derived from Zhang *et al.* (2010). Data of Catchments 15-18 were from Sun *et al.* (2014). Data of Catchments 19-21 were from Zheng *et al.* (2009), Jiang *et al.* (2015), and Gao *et al.* (2016), respectively. I used the change points given in the literatures to divide the observation period into the reference and elevation periods. The LI method further divides the evaluation period into a number of subperiods. The column “The Last Subperiod” denotes the last one, which was used as the evaluation period for the total differential method, the decomposition method and the complementary method. The bold and italic rows denote that the column “Evaluation Period” is the same as the column “The Last Subperiod”.

^bCatchments 1-14 are in Ausralia and the others in China. 1: Adjungbilly CK; 2: Batalling Ck; 3: Bombala River; 4: Crawford River; 5: Darlot Ck; 6: Eumeralla River; 7: Goobarragandra CK; 8: Jingellic CK; 9: Mosquito CK; 10: Pine Ck; 11: Red Hill; 12: Traralgon Ck; 13: Upper Denmark River; 14: Yate Flat Ck; 15: Yangxian station, Hang River; 16: Ankang station, Hang River; 17: Baihe station, Hang River; 18: Danjiangkou station, Hang River; 19: Headwaters of the Yellow River Basin; 20: Wei River; 21: Yan River.

637
638
639
640
641

Table 2. Comparisons of R (mm yr⁻¹), P (mm yr⁻¹), E_0 (mm yr⁻¹), and n (dimensionless) between the reference and the evaluation periods^a

Catchment No.	R_1	R_2	P_1	P_2	E_{01}	E_{02}	n_1	n_2	ΔR	ΔP	ΔE_0	Δn
1	223	216	959	1038	950	928	2.7	4.1	-7.2	79.2	-21	1.4
2	40.6	31	655	629	1087	1087	3	3.2	-9.7	-27	0	0.2
3	249	127	847	736	780	780	2.3	3.2	-122	-112	0.4	0.9
4	90.6	41.5	753	685	1002	989	2.9	3.7	-49	-67	-13	0.8
5	94.9	46.3	718	633	1000	992	2.5	3	-49	-85	-9	0.5
6	70.8	34.3	756	687	989	987	3.4	4.1	-36	-69	-2	0.6
7	575	406	1123	995	931	957	1.1	1.4	-169	-128	25	0.3
8	139	139	871	821	1043	1008	2.7	2.5	-0.4	-50	-35	0
9	24.1	19.2	659	621	1100	1067	3.7	3.8	-4.9	-37	-33	0.1
10	116	24.3	588	638	927	958	1.7	4.2	-92	50.4	31	2.5
11	297	68	986	716	884	905	2.3	3.6	-229	-271	22	1.3
12	301	265	992	956	820	828	2.7	2.8	-36	-36	7.4	0.1
13	48.5	32.6	752	725	991	1021	4.2	4.4	-16	-28	30	0.2
14	90.4	52.6	753	739	991	1015	2.9	3.7	-38	-14	24	0.8
15	435	295	948	795	1008	1047	1.1	1.2	-139	-153	38	0.1
16	520	353	1035	894	1074	1109	1	1.2	-167	-141	35	0.2
17	441	291	939	820	1149	1182	1	1.2	-151	-119	33	0.2
18	412	296	913	821	1163	1179	1	1.1	-116	-92	15	0.2
19	180	144	512	491	774	751	1.1	1.3	-36	-21	-23	0.2
20	90.2	52.1	585	520	895	908	2.1	2.3	-38	-65	13	0.2
21	37.7	24.6	521	462	954	995	2.6	2.5	-13	-59	41	0

642 ^aThe subscript "1" denotes the reference period and "2" denotes the evaluation period. $\Delta X = X_2 - X_1$ (X as
643 a substitute for R , P , E_0 , and n).
644
645
646
647
648
649
650
651
652
653
654
655
656
657

658
659
660
661
662
663

Table 3. Effects of precipitation (ΔR_P , mm yr⁻¹), potential evapotranspiration (ΔR_{E_0} , mm yr⁻¹), and catchment (ΔR_n , mm yr⁻¹) changes (ΔR_n , mm yr⁻¹) on the mean annual runoff resulting from the four methods

域代码已更改

Catchment NO. ^a	LI Method			Decomposition Method	Total Differential Method			Complementary Method		
	ΔR_P	ΔR_{E_0}	ΔR_n	ΔR_n	ΔR_P	ΔR_{E_0}	ΔR_n	ΔR_P	ΔR_{E_0}	ΔR_n
1	-70.9	-8.99	-24.3	-44.6	-67	4.82	-62	-60.7	4.34	-47.3
2	-6.49	0.95	-9.74	-9.65	-7.2	1.3	-13	-6.23	1.13	-10.2
3	-89	25.9	-140	-128	-104	26.6	-483	-88	25.7	-140
4	-18.1	2.09	-35.4	-36.3	-18	2.37	-58	-14.8	1.99	-38.5
5	-27.9	1.14	-21.3	-18.6	-34	1.18	-27	-28.1	0.97	-20.9
6	-19.9	0.29	-16.7	-14.9	-24	0.36	-22	-19.9	0.29	-16.7
7	-211	-7.19	-101	-90.9	-236	-6.9	-134	-211	-6.21	-102
8	-32.2	12.3	-14.4	-12.6	-35	12.6	-15	-32.9	11.9	-13.3
9	-11.8	3.02	-9.96	-8.45	-13	0.85	-20	-8.76	0.56	-10.5
10	19.47	-5.61	-119	-96.5	0.91	-10	-291	0.56	-6.53	-99.1
11	-150	-7.46	-71.8	-60.7	-188	-9.4	-113	-144	-7.04	-78.3
12	-9.88	-3.99	-79.2	-82	-11	-0.5	-154	-10.8	-0.57	-81.6
13	-6.98	-4.36	-4.54	-4.21	-8	-5.1	-5.2	-7	-4.38	-4.51
14	-4.84	-4.42	-28.7	-27.9	-5.6	-5	-37	-4.85	-4.4	-28.6
15	-104	-8.56	-24.8	-23	-110	-9.4	-27	-103	-8.52	-25.1
16	-99.3	-7.99	-58.8	-56	-105	-8.3	-68	-99	-7.92	-59.1
17	-78.8	-6.26	-63.9	-61	-84	-6.5	-76	-78.6	-6.2	-64.2
18	-60.1	-2.79	-53.5	-52	-64	-2.9	-62	-60	-2.77	-53.6
19	-11.9	3.89	-27.6	-27	-12	3.81	-31	-11.9	3.85	-27.5
20	-27.5	-2.46	-18.5	-17	-31	-4.4	-26	-25.5	-3.47	-19.5
21	-10.4	-3.47	-2.11	-3.4	-9.9	-4.8	-4.8	-8.27	-3.86	-3.82

^aThe bold and italic numbers denote that the evaluation period of the catchment comprised/comprises a single subperiod.

664
665
666
667
668
669
670
671
672
673
674
675

676
677
678
679
680

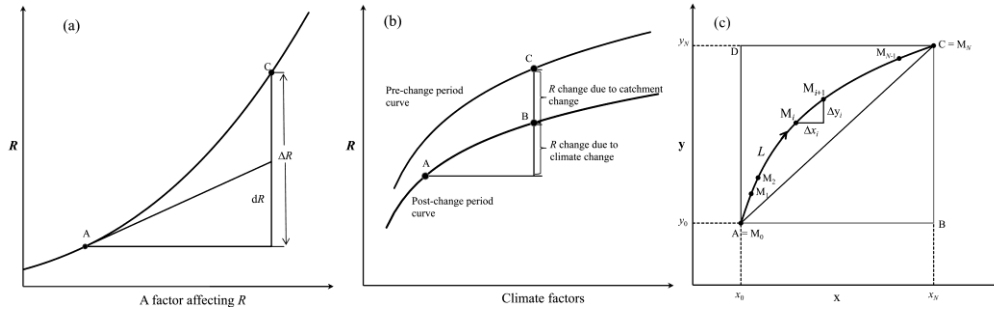
Table 4. Comparisons of the path-averaged with the point sensitivities of runoff^{a, b}

Catchment NO.	$\bar{\lambda}_P$	$\bar{\lambda}_{E_0}$	$\bar{\lambda}_n$	λ_{Pf}	λ_{E_0f}	λ_{nf}	λ_{Pb}	λ_{E_0b}	λ_{nb}
1	0.68	-0.55	-17	0.621	-0.39	-71.8	0.497	-0.32	-39.7
2	0.2	-0.08	-27.3	0.227	-0.1	-30.9	0.168	-0.07	-19.6
3	0.58	-0.36	-26.7	0.68	-0.42	-79	0.473	-0.39	-6.29
4	0.3	-0.16	-30.5	0.39	-0.2	-50.1	0.248	-0.14	-21
5	0.33	-0.14	-43.1	0.394	-0.19	-59.4	0.264	-0.12	-33.2
6	0.29	-0.16	-26.5	0.352	-0.2	-34.9	0.228	-0.12	-19.1
7	0.71	-0.32	-223	0.781	-0.33	-299	0.615	-0.26	-157
8	0.49	-0.26	-77.9	0.478	-0.27	-64.9	0.429	-0.24	-50.7
9	0.16	-0.07	-11.8	0.161	-0.07	-17.6	0.052	-0.02	-4.31
10	0.27	-0.12	-40.9	0.45	-0.16	-99.9	0.101	-0.05	-7.8
11	0.55	-0.35	-56.1	0.695	-0.44	-88.2	0.367	-0.22	-30.7
12	0.72	-0.45	-57.3	0.74	-0.53	-61.1	0.775	-0.67	-16.7
13	0.25	-0.15	-19.8	0.29	-0.17	-22.5	0.219	-0.12	-17.1
14	0.34	-0.18	-37.2	0.393	-0.21	-48.6	0.291	-0.16	-27.8
15	0.68	-0.22	-275	0.719	-0.25	-303	0.635	-0.2	-246
16	0.7	-0.23	-326	0.745	-0.24	-378	0.659	-0.21	-279
17	0.66	-0.19	-320	0.708	-0.2	-378	0.609	-0.18	-267
18	0.65	-0.19	-315	0.692	-0.19	-363	0.614	-0.18	-270
19	0.58	-0.17	-153	0.602	-0.17	-175	0.552	-0.17	-134
20	0.32	-0.12	-50.1	0.402	-0.16	-69.6	0.255	-0.1	-37.7
21	0.2	-0.06	-29.2	0.234	-0.09	-34	0.157	-0.05	-22.6

681 ^a $\bar{\lambda}_P$ (mm mm⁻¹), $\bar{\lambda}_{E_0}$ (mm mm⁻¹), and $\bar{\lambda}_n$ (dimensionless) represent the path-averaged sensitivities of
682 runoff to precipitation, potential evaporation, and catchment properties (see Appendix D). If the
683 evaluation period comprises only one subperiod, $\bar{\lambda}_P$, $\bar{\lambda}_{E_0}$ and $\bar{\lambda}_n$ was calculated as: $\bar{\lambda}_P = \Delta R_P / \Delta P$,
684 $\bar{\lambda}_{E_0} = \Delta R_{E_0} / \Delta E_0$, and $\bar{\lambda}_n = \Delta R_n / \Delta n$. If the evaluation period comprises $N > 1$ subperiods, the equations become:
685 $\bar{\lambda}_P = \sum_{i=1}^N |\Delta R_{Pi}| / \sum_{i=1}^N |\Delta P_i|$, $\bar{\lambda}_{E_0} = -\sum_{i=1}^N |\Delta R_{E_0i}| / \sum_{i=1}^N |\Delta E_{0i}|$, and $\bar{\lambda}_n = -\sum_{i=1}^N |\Delta R_{ni}| / \sum_{i=1}^N |\Delta n_i|$, where the subscript i denotes the i th
686 subperiod.

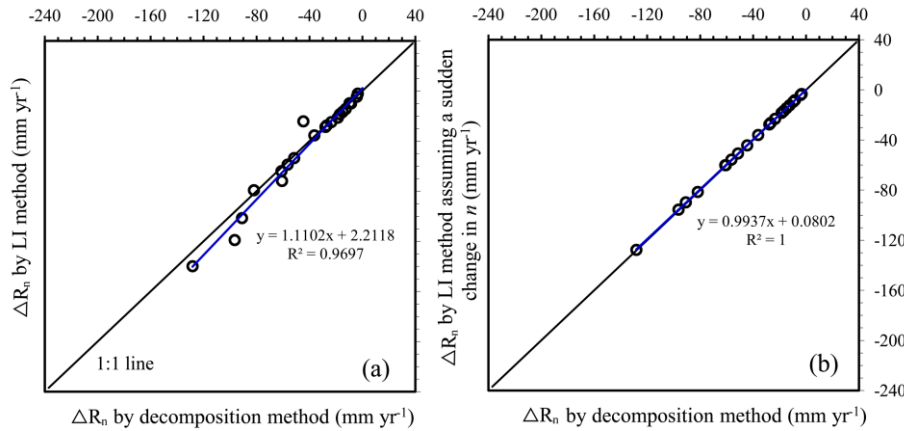
687 ^b λ_P , λ_{E_0} , and λ_n represent the point sensitivities of runoff. The subscript “ f ” represents a forward
688 approximation, i.e. substituting the observed mean annual values of the reference period into Eq. (2) to
689 calculate the sensitivities, while the subscript “ b ” represents a backward approximation (Zhou et al.,
690 2016), i.e. substituting the observed mean annual values of the evaluation period into Eq. (2).
691

692
693
694
695



696
697
698
699

Fig. 1. A schematic plot to illustrate (a) the total differential method, (b) the decomposition method, and (c) the LI method.



700
701
702
703
704
705
706
707
708
709

Fig. 2. Comparison between the LI method and the decomposition method. (a) Comparison of the estimated contribution to the runoff change from catchment change (ΔR_n); (b) the decomposition method is equivalent to the LI method that assumes a sudden change in catchment properties following climate change. In this case, the integral path of the LI method is the broken line AB+BC in Fig. 1(c) (x represents climate factors and y catchment properties, *i.e.* n) and

$$\Delta R_n = \int_{AB+BC} \frac{\partial R}{\partial n} dn = \int_{AB} \frac{\partial R}{\partial n} dn + \int_{BC} \frac{\partial R}{\partial n} dn = 0 + \int_{BC} \frac{\partial R}{\partial n} dn = \int_{n_1}^{n_2} f_n(P_2, E_{02}, n) dn$$

where the subscript "1" denotes the reference period and "2" denotes the last subperiod of the evaluation period.

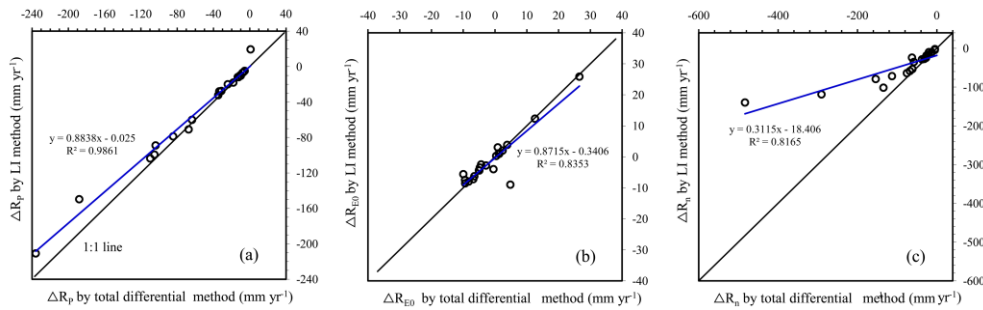


Fig. 3. Comparison of the estimated contribution to runoff from the changes in (a) precipitation (ΔR_P), (b) potential evapotranspiration (ΔR_{E_0}), and (c) catchment properties (ΔR_n) between the LI method and the total differential method.

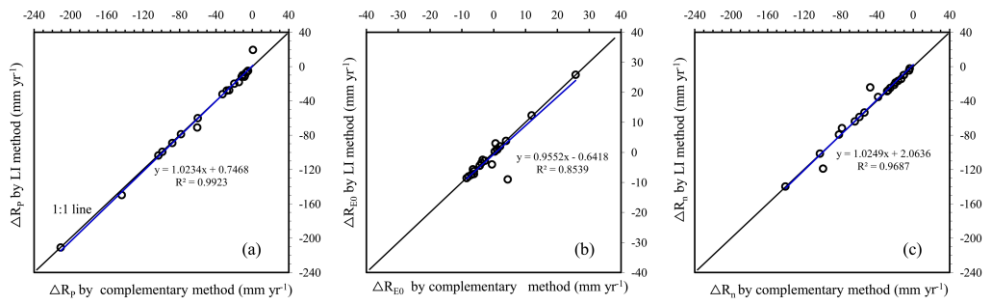


Fig. 4. Comparison of (a) ΔR_P , (b) ΔR_{E_0} , and (c) ΔR_n between the LI method and the complementary method ($a = 0.5$).

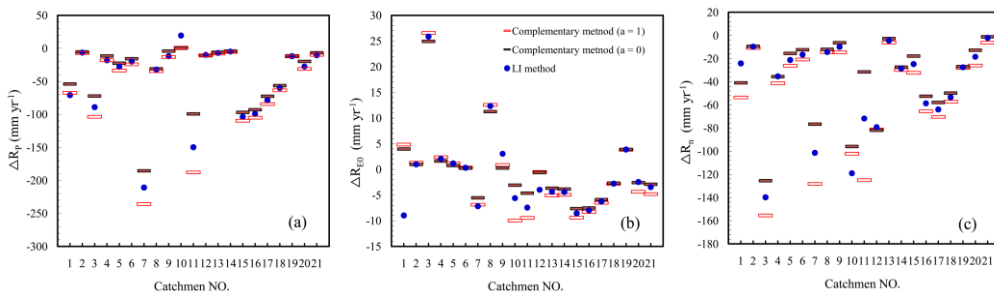


Fig. 5. Comparison of (a) ΔR_P , (b) ΔR_{E_0} , and (c) ΔR_n by the LI method with the upper ($a=1$) and lower ($a=0$) bounds given by the complementary method. According to Zhou et al. (2016), the upper and lower bounds of ΔR_P , ΔR_{E_0} , and ΔR_n are reached when a is 0 or 1.

带格式的: 字体: 非加粗

域代码已更改

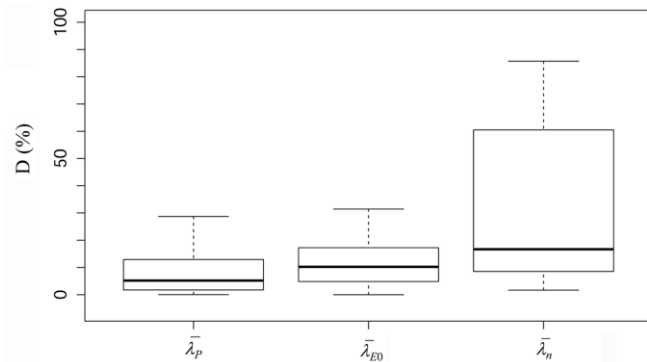
域代码已更改

带格式的: 字体: 非加粗

域代码已更改

带格式的: 字体: 小四

725
726



727
728

Fig. 6. Boxplots showing the temporal variability of the path-averaged sensitivities of water yield to precipitation ($\bar{\lambda}_p$), potential evapotranspiration ($\bar{\lambda}_{E0}$), and catchment properties ($\bar{\lambda}_n$). D (%) was calculated as the relative difference between the sensitivity of the whole evaluation period and that of a subperiod. In the calculations, I excluded the catchments whose evaluation periods were not long enough to comprise two or more subperiods. Box spans the inter-quartile range (IQR) and solid lines are medians. Whiskers represent data range, excluding statistical outliers, which extend more than 1.5IQR from the box ends.

735
736
737
738
739
740
741
742
743
744
745
746
747
748
749
750
751
752
753
754
755
756
757
758
759

760

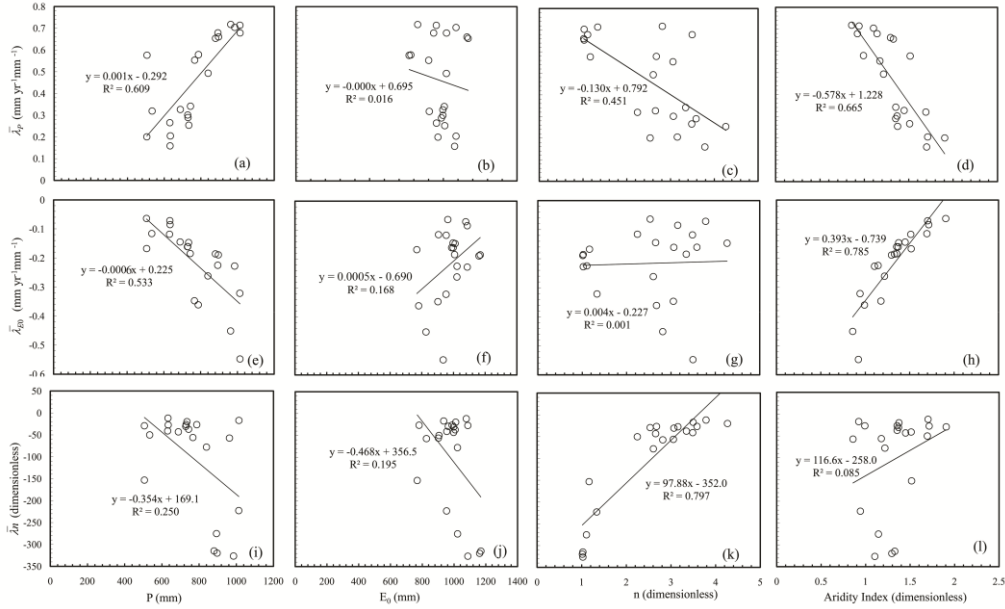


Fig. 7. $\bar{\lambda}_P$, $\bar{\lambda}_{E_0}$ and $\bar{\lambda}_n$ in correlation with P , E_0 , n , and aridity index.

761

762

763

764

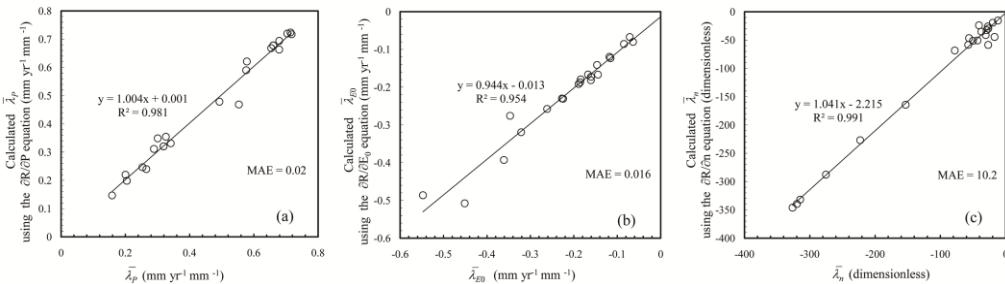


Fig. 8. Comparisons of $\bar{\lambda}_P$, $\bar{\lambda}_{E_0}$ and $\bar{\lambda}_n$ (given in Table 4) with those predicted using Eq. (2) with the

long-term mean values of P , E_0 , and n as inputs. $MAE = N^{-1} \sum_{i=1}^N |O_i - P_i|$, is the mean absolute error,

where O and P are values that actually encountered (given in Table 4) and predicted using Eq. (2) respectively, and N is the number of selected catchments.

765

766

767

768

769

770

771

772

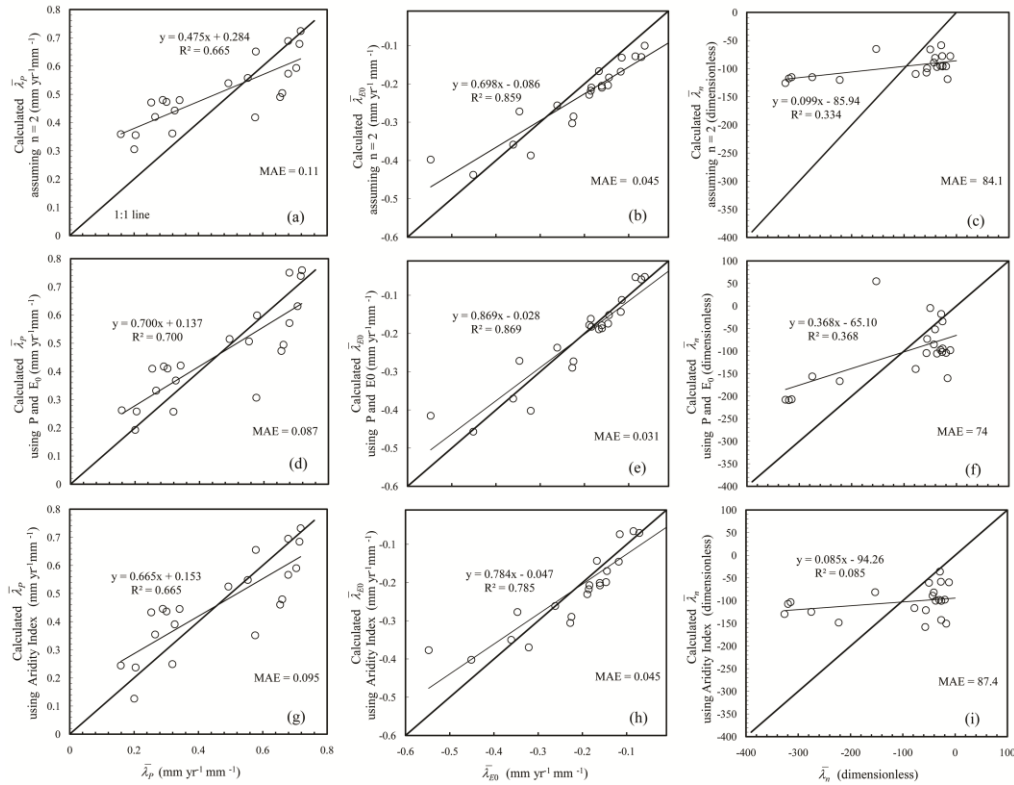
775
776
777
778
779
780
781

Fig. 9. Comparisons of $\bar{\lambda}_P$, $\bar{\lambda}_{E0}$ and $\bar{\lambda}_n$ with those predicted by the three strategies. (a)-(c) by Eq. (2) with a constant n ($n = 2$), (d)-(f) by the regression equations established using P and E_0 : $\bar{\lambda}_P = 0.0011P - 0.0006E_0 + 0.21$ ($R^2 = 0.7$), $\bar{\lambda}_{E0} = 0.0007P - 0.0007E_0 - 0.38$ ($R^2 = 0.87$), and $\bar{\lambda}_n = -0.302P - 0.372E_0 + 493$ ($R^2 = 0.37$), and (g)-(i) by the regression equations established using only the aridity index, as shown in Fig. 7 (d), (h) and (l). MAE was calculated as for Fig. 8.

782

783
784